Hyperbranched Thermosetting Poly(imide−ester): Synthesis and Properties

Kun Xu*,† and James Economy

Department of Materials Science & Engineering, University of Illinois at Urbana−Champaign, Urbana, Illinois 61801

Received September 28, 2003; Revised Manuscript Received February 16, 2004

ABSTRACT: A new family of polymer, namely hyperbranched thermosetting poly(imide−ester) (HBPIE), was successfully prepared by the esterification reaction between a hyperbranched oligoimide terminated with carboxylic end groups (−COOH) and a hyperbranched oligoester terminated with acetoxy end groups (−OAc). The hyperbranched oligoimide has a degree of branching of one, $M_w = 14\,180$, and polydispersity Pd = 1.953. The −OAc-terminated oligoester has $M_w = 7000$ and polydispersity Pd = 1.17. The NMP solution of the oligoimide and oligoester had excellent film-forming properties. HBPIE films cured from these two oligomers are thermally stable and display surface area of 83 m^2/g due to their intrinsic microporosity (pore size 12.7 Å). The submicrometer thin film of HBPIE also displays an intermediate dielectric constant and high dielectric breakdown strength.

Introduction

Polyimides are the most well-known high-temperature polymers because they have several advantages, including the excellent mechanical properties and thermoxidative stability, relatively low dielectric constant, and superior chemical resistance.[1] However, they also have some disadvantages, such as anisotropic properties in coatings, relatively poor adhesion to other substrates and to itself, medium dielectric breakdown strength, and relatively high current leakage.[2] In the past 10 years, we have been developing a family of all aromatic thermosetting copolyesters (ATSP). ATSP has excellent thermal stability (thermally stable up to 350 °C in air and 400 °C in N_2), good chemical resistance, excellent adhesion properties, low moisture pickup, and low cost and can be recycled back into oligomer form.[3] A unique property of ATSP is that self-adhesion can be carried out in the solid state between two cured coatings via interchain transesterification reaction (ITR) at the interface.[4] Consequently, ATSP has been successfully used as a matrix in thick section composites[5] and as a high-temperature adhesive.[6] Because of its cross-linked structure, ATSP provides a direct solution to the anisotropic properties associated with polyimides. In addition, ATSP has higher dielectric breakdown strength with minimum current leakage[7] and good self-adhesion via ITR.[4]

To improve properties of polyimides, it would seem advantageous to combine the two systems into one, which incorporates both polyimide and ATSP functionalities. Presumably, the copolymer should also benefit ATSP by providing a higher T_g due to the contribution from imide groups.

The following section will discuss the synthesis, characterization, and properties of the hyperbranched thermosetting copoly(imide−ester).

Experimental Section

Tris(4-nitrophenyl)amine (TNPA), 2,2-bis(3,4-dicarboxyphenyl)hexafluoropropane dianhydride (6FDA), 1,2,4-benzenetricarboxylic anhydride (BTCA), and pallidium with 10 wt % activated carbon were purchased from Aldrich. Anhydrous *N*,*N*-dimethylacetamide (DMAc) and *m*-xylene were also purchased from Aldrich. Hydrazine monohydrate (HDMH) was purchased from Acro, and 1,4-dioxane was purchased from Fisher Scientific Inc. All the chemicals were used as received.

Silicon wafers (4 in. diameter, ⟨100⟩ orientation, p-type resistance 0.0005−0.020 Ω·cm, thickness 525 ± 25 μm, single polished wafer) were purchased from Southwest Silicon Inc. TEM nickel grids for sputter shadow mask were purchased from SPI Supplies. Ceramic 8 type magnets used in the sputtering were purchased from Dexter Magnetic Technologies and were cut to the desired size using a diamond saw in the UIUC glass shop.

All glassware was cleaned thoroughly in a KOH/NaOH base bath and dried in an oven at 150 °C prior to use. The stainless steel 47 mm pressure filtration device (100 mL) and the type AW prefilter were purchased from Millipore Inc.

Thermal analyses of oligomers and polymers were done using either a TA Instruments DSC 2910 or a TGA 2950 ramped at 10 °C/min in a nitrogen atmosphere. ^{1}H NMR measurements were carried out using a Varian Unity 400 NB NMR system with DMSO-d_6 as solvent. The ^{1}H NMR data were analyzed using NUTS software. For FT-IR measurements, for samples in powder form, they were measured in diffuse reflectance mode, and the samples were ground with KBr into fine powders and dried at 150 °C in a vacuum oven overnight prior to the measurements. The molecular weight and distribution was measured using gel permeation chromatography (GPC). The characterization was performed using NMP + 0.5 M LiBr solvent in a 3× Plgel 10uM mixed B LS column at 25 °C with a Waters 515 pump. Three detectors were used including a Viscotek HR 40 refractive index detector, a Viscotek T60A dual light scattering, and a differential pressure viscometer. Polystyrene was used as a standard for the conventional calculation of the M_w. Film thickness was measured using Tecor Alpha step profilometry. The dielectric breakdown strength measurements were performed using a B&L probe station and a HP 4339B high-resistance meter. The dc voltages were applied to the sample stepwise from 0 to 200 V at 5 V/step and 5 s stay at each voltage point to allow samples to reach equilibrium. The voltage and current were recorded, and the breakdown voltage was determined as the voltage at the onset of exponential increase of current. The breakdown field was calculated from the breakdown voltage and the film thickness. The dielectric constant and dielectric loss were measured using a probe station and a HP 4284A Precision LCR meter with 0.003 V bias (at 50 V/cm biased electric field). A frequency scan was performed from 20 Hz to

† Current address: 42628 Shoreham Park Ct., Fremont, CA 94538.

* Corresponding author: Ph (510)-657-7482; Fax (810)-659-8212; e-mail kunxu2002@yahoo.com.

10.1021/ma035456q CCC: $27.50 © 2004 American Chemical Society
Published on Web 05/07/2004

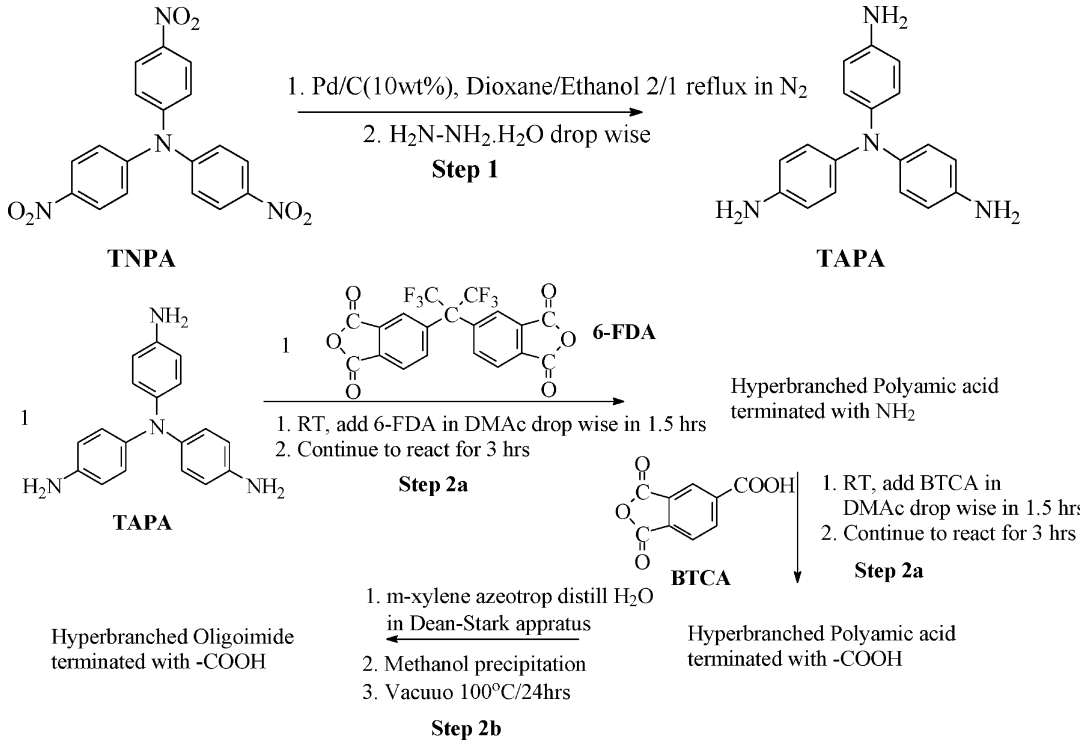

Figure 1. Synthesis of tris(4-aminophenyl)amine (step 1) and hyperbranched oligomer imide terminated with carboxylic acid group (steps 2a, 2b).

1 MHz in log step, and 300 points were measured in each scan. Both the capacitance and dielectric loss were recorded. The size of the electrode pad was measured using optical microscope. The dielectric constant was then calculated from the capacitance, film thickness, and the area of the pad. Digital Instruments MultiMode AFM was used to observe the surface topography of ATSP thin film in tapping mode. Nanodevices Metrology probe TAP 300 (resonant frequency 300 kHz and spring constant 40 N/m) was used as the probe in the AFM studies. Nanoscope III 4.43r8 offline software was used to analyze AFM image. Mass spectrometry was performed in a VG-70-VSE B with samples loaded in a direct insertion probe and electron impact ionization. Dynamic secondary ion mass spectrometry (DSIMS) was performed on a Cameca IMS-5f instrument. A Cs^+ primary ion beam (14.5 keV, 35 nA) was used to sputter through the interface at ~3 Å/s sputtering rate, with a 250 μm × 250 μm raster area and a 10 μm × 10 μm detecting area. Before loading into the SIMS chamber, samples were sputtered with a 10 Å Au layer to prevent static accumulation The analysis of surface area and micropore analysis was carried out with an Autosorb-1 volumetric sorption analyzer controlled by Autosorb-1 for Windows 1.19 software (Quantachrome Corp.). All samples were degassed at 150 °C until the outgas pressure rise rate was lower than 5 μHg/min. Nitrogen isotherm results at 77 K and carbon dioxide isotherm results at 291 K were used for surface areas calculations. Nitrogen and carbon dioxide surface areas of the samples were determined using the BET equation and Dubinin−Radushkevich (DR) equations, respectively. The CO_2 DR method was also used for micropore analysis.

Synthesis of Tris(4-aminophenyl)amine (TAPA).[8] As illustrated in Figure 1, step 1, the synthesis of TAPA was achieved by reducing TNPA using HDMH, catalyzed by C/palladium as reported in the literature and will not be repeated here.[8] The crude product was recrystallized using ethanol. For the final product: melting point 244.92 °C, 84.99 J/g (241−242 °C, lit.[8]). IR spectrum (KBr, cm^{-1}): 3411, 3340, 3211, ($-NH_2$ st) 3029 (arC−H st) 1620 (arC−C st, $-NH_2$ δ). ^{1}H NMR (DMSO-d_6) spectrum, δ (ppm): 6.60 (6H, ArH), 6.45 (6H, ArH), 4.68 (6H, NH_2).

Synthesis of Carboxylic Acid-Terminated Hyperbranched Oligoimide (HBOI). In a 1000 mL three-neck flask equipped with a magnetic stirrer, 5.22 g (18 mmol) of TAPA was dissolved in 240 mL of DMAc under a nitrogen purge to form a purple solution at room temperature (see Figure 1, step 2a reaction and setup). Then, 8 g (18 mmol) of 6FDA was dissolved in 120 mL of DMAc and added into the TAPA solution in a dropwise manner over 12 h. The solution color changed from purple to brown during the addition of 6FDA. After the addition was finished, the reaction was allowed to continue for 10 h. Then, 3.46 g (18 mmol) of BTCA was dissolved in 60 mL of DMAc and added into the reaction mixture in a dropwise manner over 6 h. The reaction was allowed to continue with stirring for 1 h after the addition was finished. Then, 180 mL of *m*-xylene was added into the reaction, and 280 mL of *m*-xylene was added to a 280 mL capacity Dean−Stark apparatus (illustrated as step 2b in Figure 1). The reaction mixture was heated at 150 °C for 18 h. The solution color changed to orange, indicating that the imidization reaction was taking place. After cooling to room temperature, the 600 mL reaction mixture was poured into 3000 mL of methanol, and a yellow powder precipitated. The crude product was collected by filtration and washed with 500 mL of methanol and dried in a vacuum at 110 °C overnight to yield 14.78 g (94.1%) of yellow powder.

The raw product was dissolved in 128.78 mL of NMP to make a 10 wt % solution and was filtered through a 0.2 μm PTFE membrane filter using pressure filtration at 20 psi. The filtrate was then poured into 1000 mL of methanol, and the precipitate was collected by filtration. The precipitate was further purified using 1 L of methanol in a Soxhlet extraction apparatus to remove any residual NMP. After 15 h of extraction, the powder was then dried in a vacuum at 150 °C for 20 h. At the end, 13.15 g of product was obtained with 83.7% yield.

Synthesis of Acetoxy-Terminated Hyperbranched Oligoester (A-1). The −OAc-terminated oligoester was synthesized by the melt polymerization of a tricarboxylic monomer, trimesic acid (TMA), a dicarboxylic monomer, isophathalic acid (IPA), a diacetoxy monomer, hydroquinone diacetate (HQDA), and acetoxybenzoic acid (ABA), a monomer containing both carboxylic and acetoxy groups, at the ratio of 2:2:7:2. The −OAc-terminated oligoester has $M_w = 7000$ and polydispersity Pd = 1.17. The synthesis and purification of oligomer A-1 and

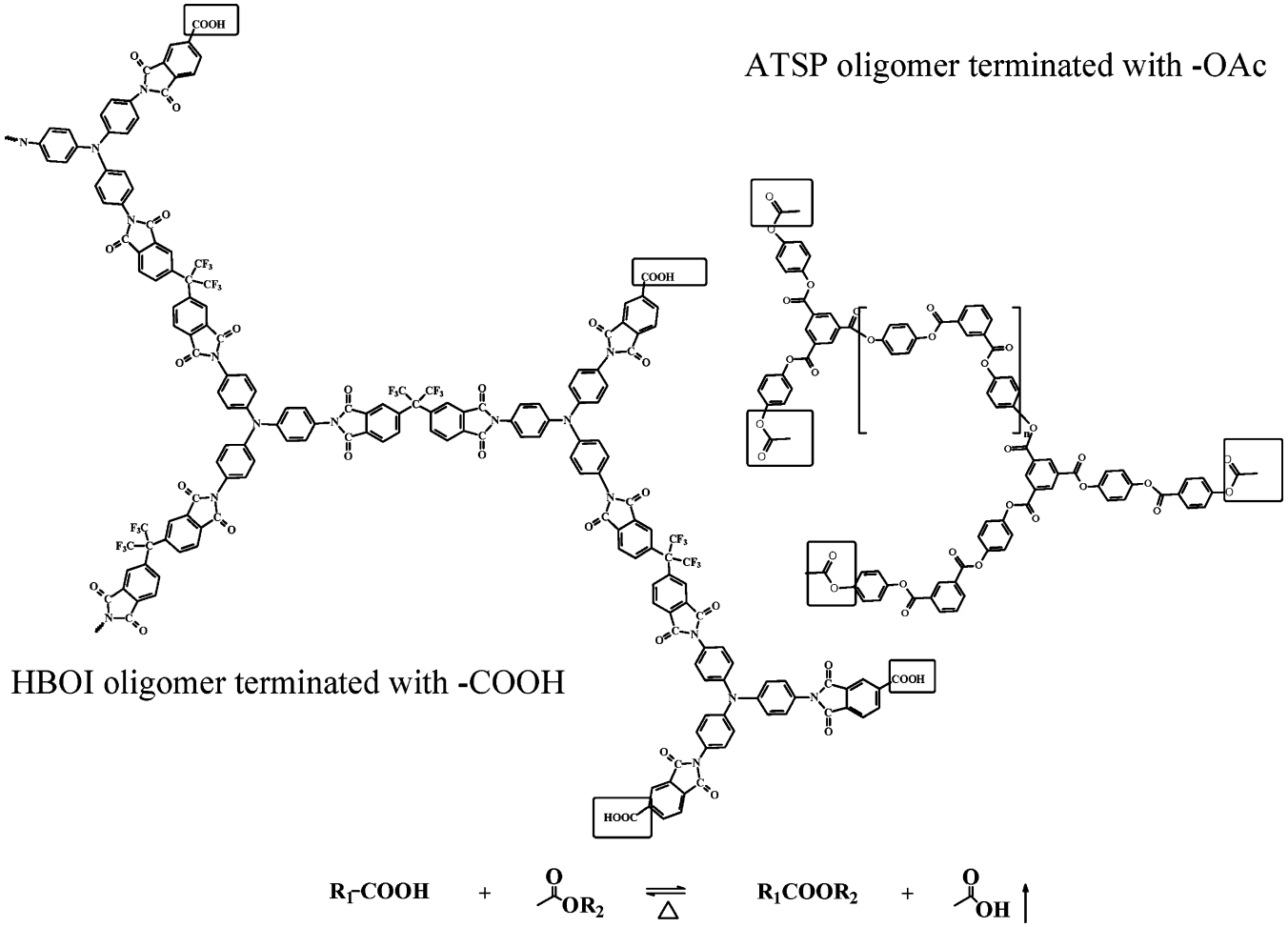

Figure 2. Cross-linking reaction between HBOI and A-1 to form HBPIE.

deuterated oligomer A-1 can be found in the literature[9] and will not be repeated here.

Fabrication of Thin Film HBPIE. Different ratios of HBOI/A-1 would give HBPIE with different amounts of end groups, which could result in different properties. But they are all processed into thin films in the same manner. For example, for HBPIE cured from HBOI and A-1 in 2/1 weight ratio, 0.67 g of HBOI and 0.33 g of A-1 were dissolved in 9 g of NMP to make a 10 g solution with solid content 10 wt %. The solution was spin-coated onto a substrate to form a thin film. The spin-coater was operated as follows: 1 s ramp from still to 1000 rpm and 1 s hold at 1000 rpm, 1 s ramp to 2000 rpm, and 1 s hold at 2000 rpm, followed by a ramp to 3000 rpm over 1 s and hold for 5 s. The coated substrate was then baked on a hot plate at 110 °C for 60 s. The resulting film was 5500 Å thick and had no observable phase separation when inspected under the optical microscope. The film was then cured at 240 °C/4 h, 280 °C/4 h, and 320 °C/4 h. When heated, the curing reaction took place between the −COOH end groups of HBOI and the −OAc end groups of oligomer A-1 (Figure 2).

Casting Thick HBPIE Film. A 5000 Å thick thin film has too little mass for those analyses that require a minimum weight. Thus, thick HBPIE was made to permit use of TGA, DSC, and surface area analysis Thick HBPIE film was cast by pouring the NMP solution of HBOI and A-1 onto a 2 in. silicon wafer, which was placed at the bottom of an aluminum disk. The solution was cured into a ∼100 μm thick film in a vacuum. These films usually shattered after curing due to the high stress induced by solvent evaporation and curing reaction, but this did not affect any of the analyses. A relatively thinner film could be obtained by spin-coating the solution at a low rpm instead of casting. About 10 μm thick film was made for IR analysis in this manner.

Processing of Dielectric Samples. A simple dry process that eliminates many of the processing steps associated with photolithography has been developed to make dielectric test samples. First, a 2270 Å thick bottom electrode was deposited by sputtering Cr (2 min) and Au (5 min) onto a silicon substrate. HBPIE was then spin-coated on the substrate. After HBPIE was cured, patterned top electrodes were obtained by sputtering Cr and Au on the cured HBPIE film using TEM nickel grid as shadow mask. During the sputtering, a TEM grid made of nickel was held in place by a ceramic-8 magnet that was taped to the backside of the silicon substrate.

Results and Discussion

Background. The structural design of the copolymer was motivated by the need for improved *processability and optimized properties*. In terms of thin film *processability*, most polymers are processed via spin-coating; hence, a polymer should be soluble to be processed in this manner. However, in most cases, neither thermoplastic aromatic polyesters nor linear polyimides are soluble. For instance, liquid crystalline copolyesters (LCP), the linear counterpart of ATSP, are only soluble in pentafluorophenol (1% solubility). This prohibits the use of LCP as a thin film in microelectronics. Alternatively, most linear polyimides, such as commonly used and commercial available polyimide PMDA−ODA, are insoluble and infusible. The polyamic acid precursor is usually processed from an NMP solution and then thermally cured to form the polyimide after coating. It is apparent that if the copoly(imide−ester) is linear, it would not be easily processed.

In terms of the *properties*, a cross-linked structure imparts isotropic properties and better thermal stability. Again, LCP, the linear counterpart of ATSP, suffers from anisotropic properties because of its rigid chain structure. Polyimides such as PMDA−ODA and BPDA−PPD have extended chain structures, resulting in anisotropic mechanical and electrical properties. In contrast, ATSP has isotropic properties. Better mechanical strength is retained even above T_g in such a system because of the cross-linked structure. Above T_g, a thermoset will only go into a leather-like state and does not flow like most thermoplastics do. Thus, more mechanical strength would be retained above T_g in thermosets. For example, in ATSP, 100% flexural modulus is still maintained at $T = 150$ °C for the ATSP matrix carbon fiber composites.[10]

Hence, to obtain better processability and properties, it was decided the copoly(imide−ester) would have a cross-linked structure and be cured from an oligomer with an imide backbone (oligoimide) and an oligomer with an ester backbone (oligoester).

Since ATSP is cured from two moderately hyperbranched oligoesters, with one oligoester terminated with −COOH and the other terminated with −OAc, an oligoimide needs to be designed so that it could react with one of the oligoester to form a cross-linked structure via esterification reaction.

In considering the structure of the oligoimide, a hyperbranched oligoimide appeared to be superior to a linear one. In most cases, a linear polyimide can only be processed via its flexible precursors—polyamic acid. To make matters worse, the polyamic acid has aging problems[11] and consequently limited shelf life. All of these would greatly complicate the curing reaction between the oligoimide and the oligoester. In contrast, a hyperbranched structure provides low viscosity and much better solubility compared to a linear structure. With a hyperbranched structure, it is possible that the oligoimide could be dissolved in NMP along with the oligoester, and the solution could be spin-coated into a thin film, which could then be cured to form a cross-linked structure. Consequently, a hyperbranched oligoimide was chosen over a linear oligoimide.

To attain the desired structures, an A2 + B3 type monomer was used to synthesize the hyperbranched oligoimide. Okamoto reported several hyperbranched oligoimides derived from an aromatic triamine and dianhydride.[12] Those oligoimides have terminal groups of either $-NH_2$ or anhydride. In our study, the synthesis was modified so that the end groups were converted from $-NH_2$ to −COOH to allow esterification reaction between the oligoimide and oligoester. The monomers needed to synthesize the oligoimide were chosen in such a way that high T_g, good solubility, and narrow M_w distribution would be expected in the oligoimide.

HBOI Oligomer: Molecular Structure and Properties. The IR (KBr, cm^{-1}) spectrum of HBOI (Figure 3) can be interpreted as follows: medium and broad bands at 3282, 3074 (COO−H st hydrogen bonded) indicate the existence of −COOH end groups; peaks at 1782 (C═O ast) 1730 (C═O st), 1375 (C−N st), and 723 (C═O bending) are representative of a polyimide structure; strong and multiple peaks around 1257 (C−F st) indicate the existence of C−F bonds. Thus, FT-IR shows the structure of HBOI as expected. However, since COO−H st and N−H st are in the same range, FT-IR could not exclude the existence of residual $-NH_2$ groups

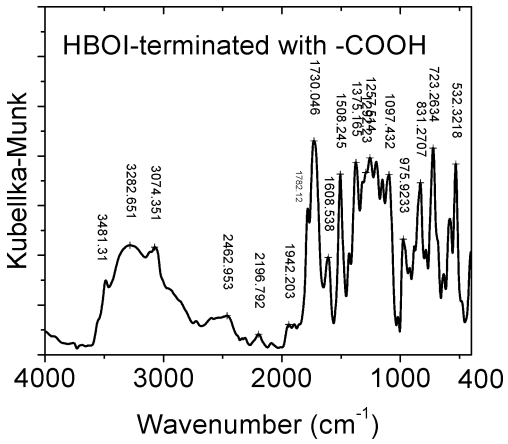

Figure 3. IR spectrum of hyperbranched oligoimide HBOI using diffuse reflectance mode.

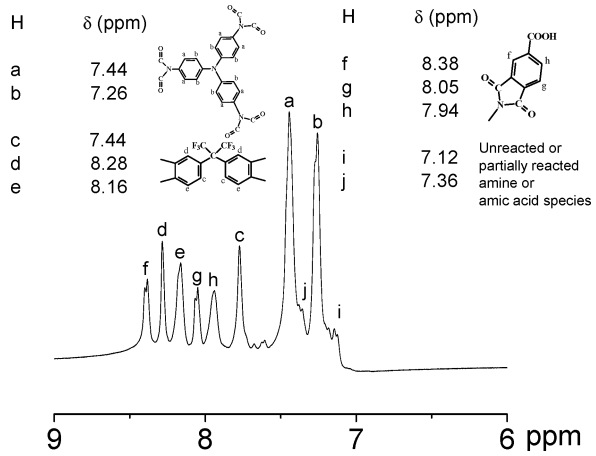

Figure 4. ^{1}H NMR spectrum of hyperbranched oligoimide HBOI.

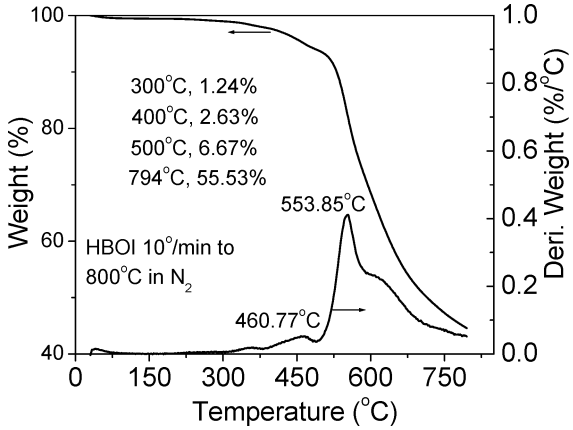

Figure 5. TGA scan of hyperbranched oligoimide HBOI.

that might not have been converted into −COOH. Fortunately, the different species can be resolved with the ^{1}H NMR spectrum. As illustrated in Figure 4, the ^{1}H NMR (DMSO-d_6), δ (ppm), spectrum can be interpreted as follows: the duplex peaks at 7.44−7.12 are representative of the protons on the benzene ring from the TAPA monomer. Peaks at 7.26 and 7.44 are the two major peaks in this regime, indicating most of the amine groups were converted to imide; that is, the oligomer is almost fully branched, and the degree of branching (DB) is close to one. Yet, there are several small peaks (at 7.12, 7.36) which may represent the unreacted or partially reacted amine or amic acid species. Peaks at

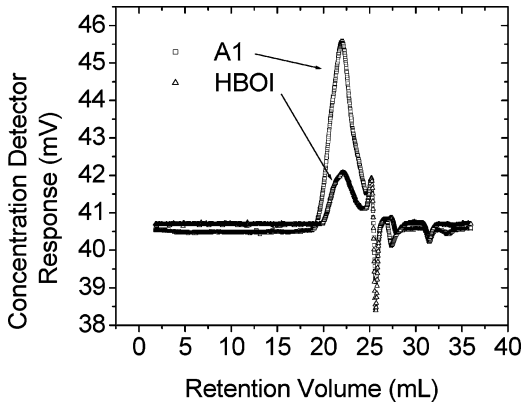

Figure 6. GPC trace of HBOI and A1.

7.77, 8.16, and 8.28 represent the three protons on the benzene of BTCA monomer, while peaks at 7.94, 8.05, and 8.38 represent the three protons on the benzene ring of 6-FDA monomer. Further, evidence that all the $-NH_2$ has been consumed is supported by the disappearance of the $-NH_2$ peak between 4 and 6 ppm.[12]

The glass transition temperature was measured as 313 °C using DSC. TGA indicates this oligoimide has an excellent thermal resistance (Figure 5); only 6.7% weight loss was observed when heating this oligomer at 10 °C/min to 500 °C in N_2.

Both HBOIE and A-1 oligomer's GPC traces are illustrated in Figure 6. For both HBOIE and A1 oligomers, there is a sharp peak right after the main peak. It could be caused by impurities with small molecular weight or an artifact due to the difference in the refractive index between the residual amount of NMP left from the purification process and the solvent NMP used in GPC. This small peak should not be included in the M_w calculation, and the M_w and M_w calculation was based on the main peak only. Using conventional calculations and polystyrene as a standard, the M_w is 14 180 with polydisperstiy 1.953 for HBOI, and the M_w is 7000 with polydispersity Pd = 1.17 for A-1. The as synthesized HBOI oligomer has a quite narrow M_w distribution for a hyperbranched material and has a smaller M_w and M_w distribution than the hyperbranched polyimides (M_w = 37 000, pd = 5.8) terminated with $-NH_2$ as reported by Okamoto.[12] This can be explained by the fact that use of BTCA as the terminating monomer and the purification process have helped to control the M_w and narrow the M_w distribution.

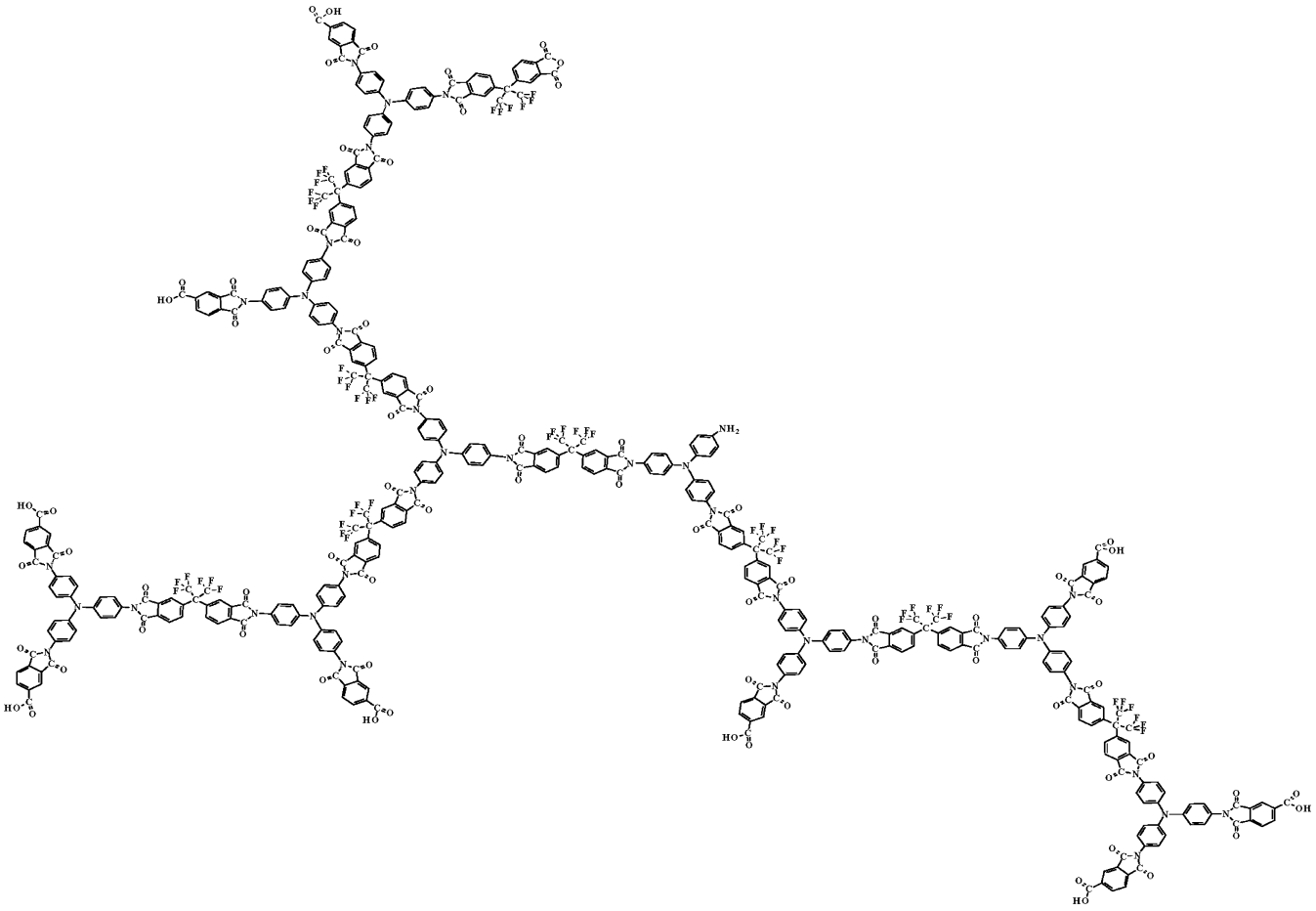

Characteristic:

1. A_2B_3 type hyper-branched polyimide terminated with –COOH
2. 1mol –COOH/873g -COOH wt %: 5.3%
3. GPC conventional method: Mn=7,262, Mw=14,180 and Pd=1.953
4. T_g=313°C

Figure 7. Possible chemical structure of hyperbranched oligoimide HBOI and its overall properties.

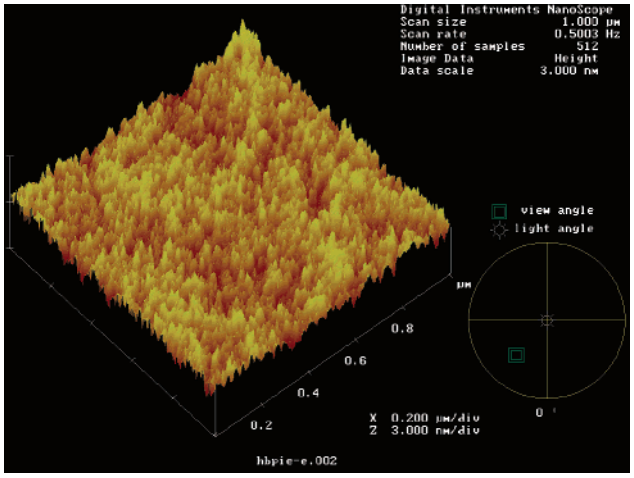

Figure 8. 1 mm × 1 mm AFM image of the surface of HBPIE film. The film is 4700 Å thick and has a mean roughness 2.8 Å over this 1 μm × 1 μm area.

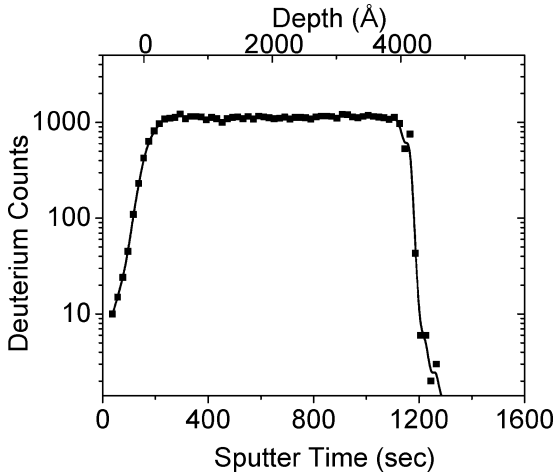

Figure 9. DSIMS spectrum of HBPIE cured from HBOI and deuterated A-1.

In Figure 7 is shown a possible chemical structure of HBOI oligomer based on GPC results and the reaction ratio of TAPA, 6-FDA, and BTCA. The percentage of −COOH groups is about 1 mol/873 g based on the excess mole of −COOH groups in the reactants.

HBPIE Film Formation. For the thin film HBPIE cured from HBOI-A1 in 2/1 ratio, there was 14.43% shrinkage in the perpendicular direction after curing. The cured film was resistant to NMP and had no observable phase separation in the $x-y$ plane when inspected using AFM in tapping mode (the surface roughness was 2.8 Å over 1 μm × 1 μm area (Figure 8). There was no observable phase separation in the z direction of HBPIE films cured from HBOI and deuterated A-1 when inspected using SIMS (Figure 9). Thus, the film is homogeneous throughout the thickness.

Curing Thin Film of HBPIE. The curing process was studied by measuring the properties of HBPIE film cured at different conditions. Along with mass spectrometry to monitor the species emitted during the curing, a picture of the curing reaction can be drawn.

Effect of the Weight Ratio of HBOI/A-1 on Curing. Presumably, dielectric breakdown strength would increase with the progress of the cross-linking of the polymer. Hence, dielectric breakdown strength was used as an index as the curing degree in HBPIE system. By using a curing profile of 240 °C for 2 h followed by 350 °C for 2 h, the dielectric breakdown strength of three HBPIE thin films of same thickness but with different ratios of HBPO and A-1 were compared (Figure 10). With HBOI/A-1 in 1/1 ratio, the highest breakdown strength of 330 V/μm was obtained, indicating the highest completion of curing among all three samples. Different degrees of curing would result in different cross-linking densities and different concentrations of polar groups left in the HBPIE film. Hence, *different ratios* of HBOI/A-1 would produce *different properties* in the cured HBPIE film and can be varied according to what type application is required for HBPIE film. For example, a higher degree of curing with the least residual polar groups would be preferred for applications of HBPIE as a dielectric material, thus using HBOI/A-1 at 1/1 ratio would be preferred over the 2/1 ratio. In contrast, when more polar groups are required, the 2/1 ratio is favored.

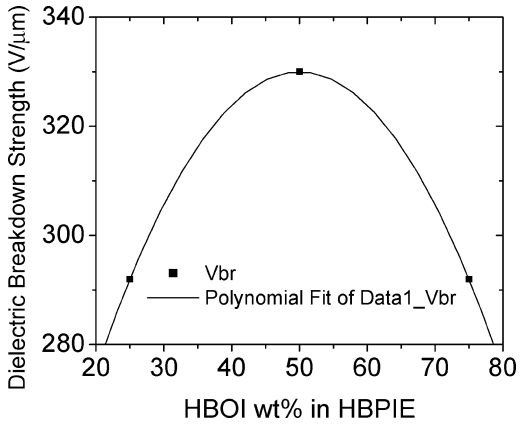

Figure 10. Dielectric breakdown strength showing a optimum value with HBOI and A-1 in 1/1 ratio by weight.

Effect of Curing Temperature on Curing Completion. Mass spectrometry was used to analyze the species emitted from powders of A-1, HBOI, and the 2/1 mixture of HBOI-A1, when heated at 5 °C/min to 330 or 380 °C in ultrahigh vacuum. The mixture of HBOI and A-1 was made by dissolution of HBOI and A-1 in NMP. Methanol was then used to precipitate the mixture; in this way, a degree of mixing close to that of the spin-coated film should be achieved.

As illustrated in Figure 11, A-1 will intrinsically have ∼4% acetic acid emitted as self-polymerization byproducts. The amount of acetic acid emitted increases in the mixture of HBOI-A-1, indicating the cross-linking between HBOI and A-1. Since HBOI has a high glass transition temperature of 313 °C, a somewhat higher temperature is required to cure HBPIE. The higher the curing temperature, the better the mobility of HBOI chains. In turn, carboxylic acid end groups would have a better chance to react with the acetoxy end groups of A-1; thus, more acetic acid would be evolved. EI-mass spectrometry has shown an increase in amount of acetic acid from 9% to 14% (Figure 12 and Figure 13), provided the final curing temperature is increased from 330 to 380 °C.

Hence, as expected, there is more complete curing at high temperature. This conclusion could also be drawn from the fact that the final film thickness decreases with the increase of final curing temperature from 300 to 400 °C (as is shown in Figure 14). Because the film thickness shrinks with curing, it can be an indicator of curing degree. Thus, the temperature at which maximum film shrinkage occurs without eroding the properties would

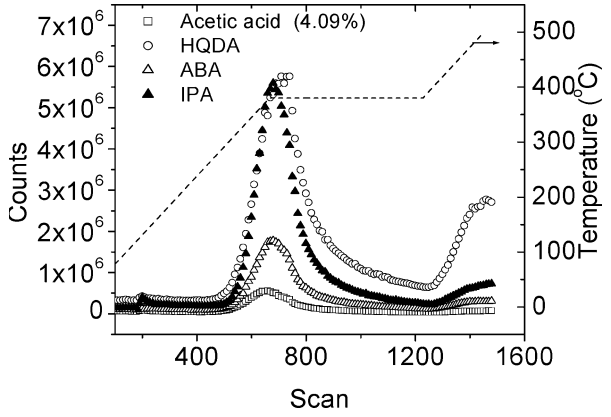

Figure 11. Mass spectrometry total ion counts for A-1 (380 °C isotherm). The curves represent the ion counts of acetic acid, HQDA, ABA, and IPA using ion mass 60, 110, 138, and 149, respectively. Scan numbers from 0 to 669 represent the first ramp to 380 °C at 5 °C/min during the initial 0-70 min, 669−1228 represents the 1 h isothermal at 380 °C, and 1228−1451 represents the second ramp to 500 °C at 5 °C/min. The 4.09% is the percentage of the ion counts of acetic acid over the total ion counts of all four species based on the integration of ion counts between scan number 400 and 1100.

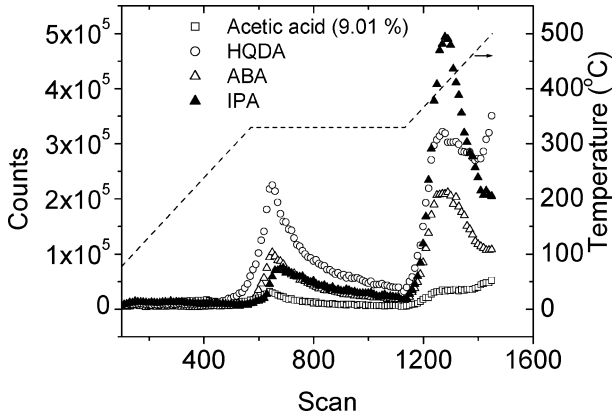

Figure 12. Mass spectrometry total ion counts for mixture of HBOI and A-1 (330 °C isotherm). The curves represent ion counts of acetic acid, HQDA, ABA, and IPA using ion mass 60, 110, 138, and 149, respectively. Scan numbers from 0 to 578 represent the ramp to 330 °C at 5 °C/min during the initial 0−70 min, 578−1126 represents the 1 h isothermal at 330 °C, and 1126−1445 represents the second ramp to 500 °C at 5 °C/min. The value 9.01% is the percentage of the ion counts of acetic acid over the total ion counts of all four species based on the integration of ion counts between scan number 400 and 1000.

be the optimum curing temperature. There is no observable degradation of the performance in HBPIE if cured up to 400 °C as indicated by the dielectric breakdown strength (Figure 15). However, when cured at 420 °C, some roughening of the surface has been observed. This suggests that 400 °C is the maximum curing temperature.

As a general feature of hyperbranched polymers in cross-linking reactions, a high functionality number can lead to too fast a cross-linking reaction and freezing of the chain before all reactive functional groups had a chance to react.[13] For the maximum possible degree of cross-linking in HBPIE, it is desirable to use a stepwise curing beginning at a temperature just above the T_g of HBOI (313 °C) to allow enough time for increased chain mobility and reaction and then proceeding to higher temperatures to drive the reaction to completion (Figure 16).

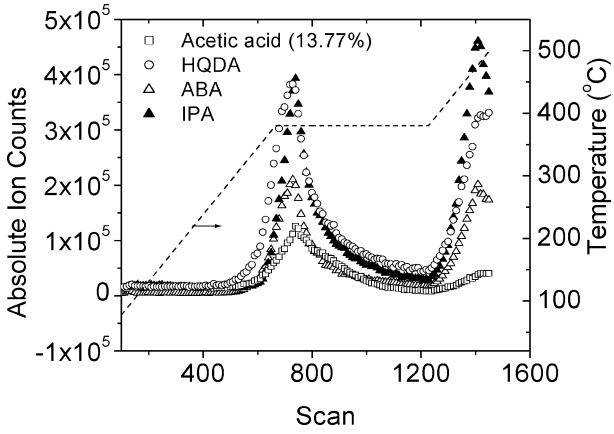

Figure 13. Mass spectrometry total ion counts for mixture of HBOI and A-1 (380 °C isotherm). The curves represent ion counts of acetic acid, HQDA, ABA, and IPA using ion mass 60, 110, 138, and 149, respectively. Scan numbers from 0 to 669 represent the ramp to 380 °C at 5 °C/min during the initial 0−70 min, 669−1228 represents the 1 h isothermal at 330 °C, and 1228−1451 represents the second ramp to 500 °C at 5C/min. The value 13.77% listed represents the percentage of the ion counts of acetic acid over the total ion counts of all four species based on the integration of ion counts between scan number 400 and 1200.

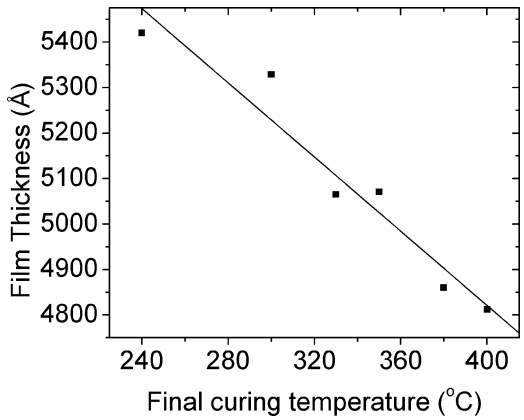

Figure 14. Relationship between film thickness and final curing temperature for HBPIE.

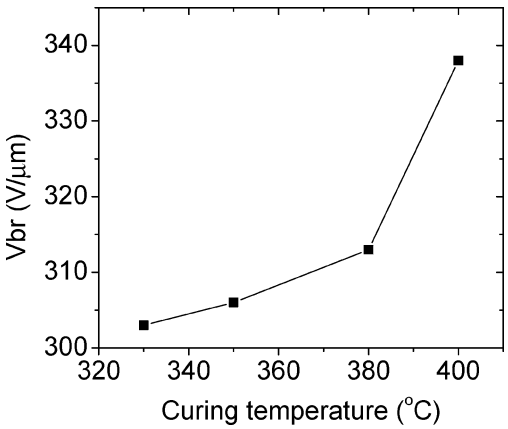

Figure 15. Relationship between dielectric breakdown strength and final curing temperature.

Properties of HBPIE. Shown in Figure 17 is the FT-IR spectrum of the cured HBPIE film on silicon (2/1 weight ratio). In comparing it with that of oligomer HBOI powder (Figure 18), the intensity of the −COOH groups C−H st was greatly reduced, indicating the consumption of −COOH groups. However, there was

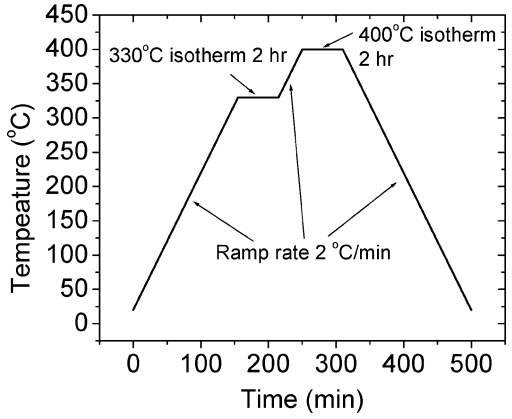

Figure 16. Stepwise cure cycle for the cross-linking of HBOI with A-1 to form HBPIE.

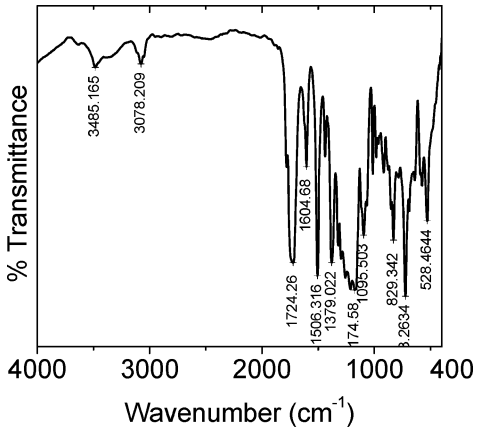

Figure 17. FT-IR spectrum of cured HBPIE film on silicon using transmittance mode.

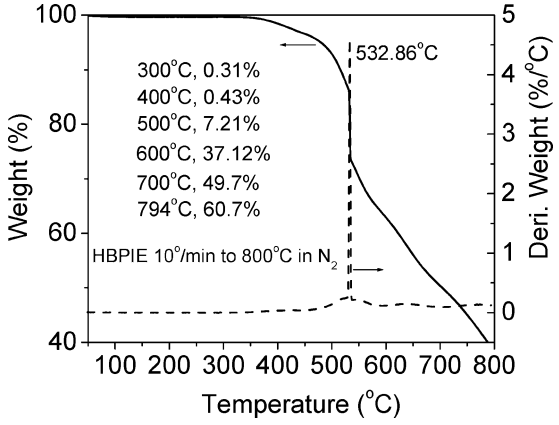

Figure 18. TGA scan of cured HBPIE film.

still small band at 3485 cm^{-1}, suggesting there was some residual −COOH groups, possibly due to the unbalanced ratio of HBOI over A-1 or even possibly incomplete curing.

Thermal Properties. As illustrated in Figure 19, with only 7% weight loss when heated to 500 °C, the cured HBPIE film has a somewhat improved thermal stability over ATSP and is similar to that of HBOI oligomer.

Surface Area. With the hyperbranched structure of both HBOI and A-1, one would expect a fairly large amount of stable space between the chain branchings, which could increase the void volume and surface area. The surface area of HBOI, A-1, and the cured HBPIE (2/1 weight ratio of HBOI/A-1) were measured using

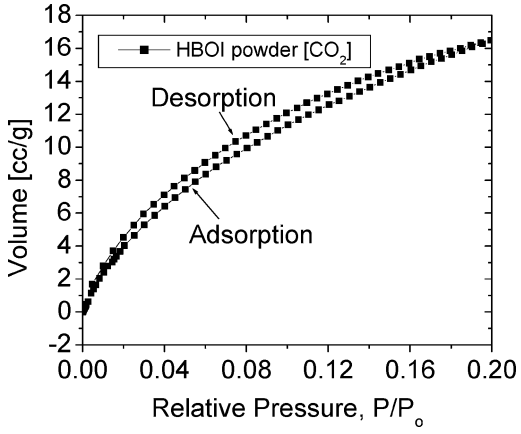

Figure 19. Carbon dioxide adsorption−desorption isotherms for HBOI powder sample at 291 K.

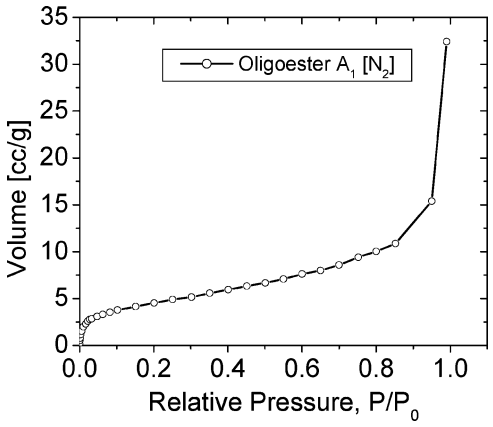

Figure 20. Nitrogen adsorption isotherms for A-1 powder sample at 77 K.

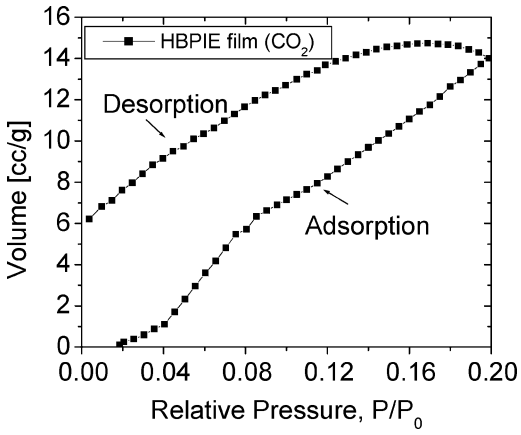

Figure 21. Carbon dioxide adsorption−desorption isotherms for HBPIE film sample at 291 K.

Table 1. Surface Area Measurements of HBOI, A-1, and Cured HBPIE Characteristics

samples	HBOI powder (CO_2-DR)	A-1 powder (N_2-BET)	cured HBPIE film (~100 μm thick) (CO_2-DR and N_2-BET)
surface area (m^2/g)	84.17	15.85	83.20 (12.7 Å pore diameter and 3.6% pore volume fraction)

both N_2 isotherm and CO_2 isotherm (Figure 20 and Figure 21). The results (Table 1) from both methods were consistent. The results would seem to indicate the hyperbranched structure of HBOI and A-1 provides for a certain degree of porosity in HBPIE. This is consistent

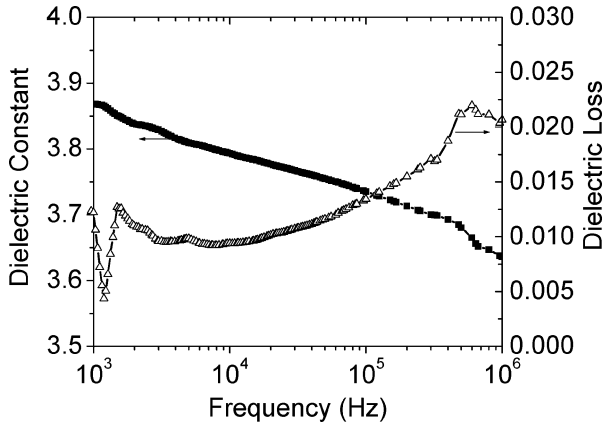

Figure 22. Frequency scan of dielectric constant and dielectric loss of HBPIE thin film. This HBPIE film was 5065 Å thick and was cured at 330 °C for 2 h.

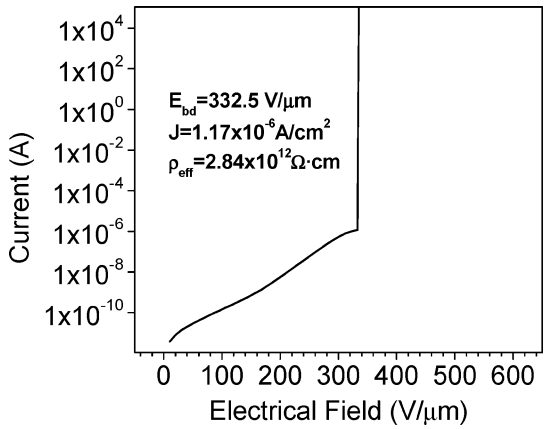

Figure 23. Dielectric breakdown of HBPIE film. This HBPIE thin film is 4812 Å thick and was cured at 330 °C for 2 h and annealed at 400 °C for 2 h.

with the literature that membranes of hyperbranched polymers could be used for gas separation.[14]

Further, the fact that the cured HBPIE in film format has similar surface area as that of HBOI powder suggests HBOI reacted well with A-1, and the cross-linking introduced additional surface area. Had it not, the surface area of HBPIE would have been much lower due to the phase-separated HBOI and A-1 species contributing to the surface area measurement individually. The apparent surface area of HBPIE would have been a weight-average of HBOI and A-1 species (~61.40 m^2/g).

Dielectric Properties of HBPIE Thin Film. The dielectric properties of HBPIE were characterized from a cured film of 2/1 weight ratio of HBOI/A-1. The dielectric constant of cured HBPIE was measured at 3.6 ± 0.2, a comparable value as that of the ATSP thin film (Figure 22). The dielectric loss is smaller than that of ATSP film due to the more rigid structure in HBOI (replace ester linkage with imide). With the increased amount of HBOI in the copolymer, the dielectric loss decreases. The dielectric breakdown strength was measured at 330 V/μm with a minimum current leakage. The performance is between that of commercial PI and that of ATSP (Figure 23). It should be noted the values reported here were based on an unoptimized weight ratio of HBOI/A-1. It would be expected that improved dielectric properties should be achieved with an optimized weight ratio and optimized curing.

For applications of HBPIE as a dielectric material, a more complete consumption of polar end groups is preferred. While a 2/1 ratio of HBOI/A-1 was used to study the curing, a more even ratio should be used to achieve the highest degree of curing. For this reason, a better understanding of the curing reaction between HBOI and A-1 is needed to further decrease the dielectric constant.

Summary

A hyperbranched poly(imide ester) (HBPIE) was successfully prepared by the esterification reaction between a hyperbranched oligoimide terminated with carboxylic end groups (−COOH) and a hyperbranched oligoester terminated with acetoxy end groups (−OAc). The synthesis of the −COOH-terminated hyperbranched oligoimide involved the formation of a hyperbranched polyamic acid via the condensation polymerization of a triamine monomer, tris(4-aminophenyl)amine (TAPA), a dianhydride, 2,2-bis(3,4-dicarboxyphenyl)hexafluoropropane dianhydride (6FDA), and an anhydride 1,2,4-benzenetricarboxylic anhydride (BTCA) at the ratio of 1:1:1 and the imidization reaction of the polyamic acid at elevated temperature. From ^{1}H NMR analysis, the hyperbranched oligoimide was found to have a degree of branching of one. The M_w was determined with GPC to be 14 180, and the M_w distribution was narrow (Pd = 1.953). The NMP solution of the oligoimide and oligoester had excellent film-forming properties. HBPIE films cured from these two oligomers (2/1 weight ratio of oligoimde vs oligoester) are thermally stable with only 7% weight loss if heated to 500 °C. They display a surface area of 83 m^2/g with an average pore diameter of 12.7 Å and pore volume fraction of 3.6%. For a 0.5 μm thick HBPIE film, the dielectric constant, dielectric loss, and breakdown strength were 3.6 ± 2, 0.02, and 330 V/μm, respectively. The HBPIE thin film could find potential applications as gas separation membranes or dielectric thin films in capacitors.

To better exploit the various possible applications of HBPIE, quantitative curing studies are necessary to understand the details of curing. Only then can we fully know how to control the degree of cross-linking, the percentage of the polar groups, and the microporosity in the cured HBPIE. Still untapped are the various other properties and applications of this new polymer; for example, the fundamental ability of HBPIE to bond with itself via ITR in the solid state opens up the same possibilities available with ATSP. One promising area for this copolymer system would be the study of water permeability, water reflux, and reverse osmosis salt rejection through thin films of HBPIE.

In conclusion, HBPIE is an elegant example of an aromatic thermosetting polymer that addresses some of the problems of using polyimides and ATSP in thin film applications. But, it should be kept in mind that the architecture and variety of functional groups are not limited to this particular system and could be easily engineered to different requirements of properties and structure.

Acknowledgment. This work was supported by DARPA DSO (Contract DABT63-97-C-0069). The thin film analysis was carried out in the Center for Microanalysis of Materials, University of Illinois, which is partially supported by the U.S. Department of Energy under Grant DEFG02-91-ER45439. The authors thank

the following staff at the Center for Microanalysis of Materials for their assistance in various analytical metrologies: Judy Baker for the DSIMS, Nancy Finnegan and Jim Mabon for the AFM. The authors also thank Liqiang Zhou at the Mass Spectrometry Lab in the School of Chemical Science and Engineering, University of Illinois, for performing the EI-mass spectrometry and Larry Markoski in Professor Jeff Moore's group at the Chemistry Department, University of Illinois, for his help on GPC. Finally, the authors thank Dr. Deli Wang in the Materials Science and Engineering Department of University of California at Santa Barbara for his valuable discussion.

References and Notes

(1) Mittal, K. L. E. *Polyimides: Synthesis, Characterization, and Applications 1−2*; Plenum Press: New York, 1984.
(2) Brown, H. R.; Yang, A. C. M.; Russell, T. P.; Volksen, W.; Kramer, E. J. *Polymer* **1988**, *29*, 1807−1811.
(3) Andreopoulos, A. G.; Economy, J. *Polym. Adv. Technol.* **1996**, *7*, 561−570.
(4) Frich, D.; Hall, A.; Economy, J. *Macromol. Chem. Phys.* **1998**, *199*, 913−921.
(5) Lopez, A.; Economy, J. *Polym. Compos.* **2001**, *22*, 444−449.
(6) Frich, D.; Economy, J.; Goranov, K. *Polym. Eng. Sci.* **1997**, *37*, 541−548.
(7) Selby, J. C.; Shannon, M. A.; Xu, K.; Economy, J. *J. Micromech. Microeng.* **2001**, *11*, 672−685.
(8) Miller, R. D.; Burland, D. M.; Jurich, M.; Lee, V. Y.; Moylan, C. R.; Thackara, J. I.; Twieg, R. J.; Verbiest, T.; Volksen, W. *Macromolecules* **1995**, *28*, 4970−4974.
(9) Xu, K. Ph.D. Thesis, University of Illinois at Urbana−Champaign, Urbana, IL, 2002.
(10) Frich, D. Ph.D. Thesis, University of Illinois at Urbana−Champaign, Urbana, IL, 1996.
(11) Kreuz, J. A.; Goff, D. L. *Mater. Res. Soc. Symp. Proc.* **1991**, 11−21.
(12) Fang, J.; Kita, H.; Okamoto, K. *Macromolecules* **2000**, *33*, 4639−4646.
(13) Voit, B. *J. Polym. Sci., Part A: Polym. Chem.* **2000**, *38*, 2505−2525.
(14) Fang, J.; Kita, H.; Okamoto, K. *J. Membr. Sci.* **2001**, *182*, 245−256.

MA035456Q